AFRL-PR-WP-TP-2003-205

FLUX-PINNING OF $Bi_2Sr_2CaCu_2O_{8+d}$ HIGH T_C SUPERCONDUCTING TAPES UTILIZING $(Sr,Ca)_{14}Cu_{24}O_{41+d}$ AND $Sr_2CaAl_2O_6$ DEFECTS

T. Haugan, W. Wong-Ng, L. P. Cook, L. Swartzendruber, H. J. Brown, and David T. Shaw

OCTOBER 2003

Approved for public release; distribution is unlimited.

PROPULSION DIRECTORATE
AIR FORCE RESEARCH LABORATORY
AIR FORCE MATERIEL COMMAND
WRIGHT-PATTERSON AIR FORCE BASE, OH 45433-7251

REPORT DOCUMENTATION PAGE

Form Approved
OMB No. 0704-0188

1. REPORT DATE *(DD-MM-YY)*	2. REPORT TYPE	3. DATES COVERED *(From - To)*
October 2003	Journal Article Preprint	

4. TITLE AND SUBTITLE

FLUX-PINNING OF $Bi_2Sr_2CaCu_2O_{8+\delta}$ HIGH T_c SUPERCONDUCTING TAPES UTILIZING $(Sr,Ca)_{14}Cu_{24}O_{41+\delta}$ AND $Sr_2CaAl_2O_6$ DEFECTS

5a. CONTRACT NUMBER
In-house

5b. GRANT NUMBER

5c. PROGRAM ELEMENT NUMBER
N/A

6. AUTHOR(S)

T. Haugan (AFRL/PRPG)
W. Wong-Ng and L. P. Cook (Division of Ceramics, NIST)
L. Swartzendruber and H. J. Brown (Division of Metallurgy, NIST)
David T. Shaw (State University of New York at Buffalo)

5d. PROJECT NUMBER
N/A

5e. TASK NUMBER
N/A

5f. WORK UNIT NUMBER
N/A

7. PERFORMING ORGANIZATION NAME(S) AND ADDRESS(ES)

Power Generation Branch (AFRL/PRPG)
Power Division
Propulsion Directorate
Air Force Research Laboratory, Air Force Materiel Command
Wright-Patterson Air Force Base, OH 45433-7251

Division of Ceramics, NIST

Division of Metallurgy, NIST

State University of New York at Buffalo

8. PERFORMING ORGANIZATION REPORT NUMBER
AFRL-PR-WP-TP-2003-205

9. SPONSORING/MONITORING AGENCY NAME(S) AND ADDRESS(ES)

Propulsion Directorate
Air Force Research Laboratory
Air Force Materiel Command
Wright-Patterson Air Force Base, OH 45433-7251

10. SPONSORING/MONITORING AGENCY ACRONYM(S)
AFRL/PRPG

11. SPONSORING/MONITORING AGENCY REPORT NUMBER(S)
AFRL-PR-WP-TP-2003-205

12. DISTRIBUTION/AVAILABILITY STATEMENT
Approved for public release; distribution is unlimited.

13. SUPPLEMENTARY NOTES
To be published in Ceramics Transactions, Vol. 104, 2000.

14. ABSTRACT

Efforts to improve the magnetic flux-pinning properties of $Bi_2Sr_2CaCu_2O_{8+\delta}$/Ag (2212/Ag) tape conductors utilizing $(Sr_{1-x}Ca_x)_{14}Cu_{24}O_{41+\delta}$ and $Sr_2CaAl_2O_6$ defects are described. Precursor powders with composition (2212 + N% volume fraction $Sr_{10}Ca_4Cu_{24}O_{41+\delta}$; N = 0, 7, 15) were prepared by solid-state reaction to obtain subsolidus phase equilibrium at 860°C, as measured by X-ray diffraction (XRD). Nanophase (10 – 20 nm) Al_2O_3 was added (1.1% mass fraction) to N = 0 and 15 fully reacted powders. Brush-on coated tapes (13 – 17 μm 2212 thickness) were processed by a partial-melt growth method in air with variable melting from 865°C to 890°C, and slow-cool recrystallization from 856°C to 847°C. The effect of different melt temperatures and compositions on film properties (phase assemblages, orientations, and compositions, and defect sizes) was studied by XRD, scanning electron microscopy (SEM), and energy dispersive spectroscopy (EDS).

15. SUBJECT TERMS

16. SECURITY CLASSIFICATION OF:			17. LIMITATION OF ABSTRACT:	18. NUMBER OF PAGES	19a. NAME OF RESPONSIBLE PERSON (Monitor)
a. REPORT	b. ABSTRACT	c. THIS PAGE			Lt. Justin Tolliver
Unclassified	Unclassified	Unclassified	SAR	20	19b. TELEPHONE NUMBER *(Include Area Code)* (937) 255-6343

Standard Form 298 (Rev. 8-98)
Prescribed by ANSI Std. Z39-18

FLUX-PINNING OF $Bi_2Sr_2CaCu_2O_{8+\delta}$ HIGH T_c SUPERCONDUCTING TAPES UTILIZING $(Sr,Ca)_{14}Cu_{24}O_{41+\delta}$ and $Sr_2CaAl_2O_6$ DEFECTS

T. Haugan, W. Wong-Ng, L. P. Cook
Division of Ceramics, Materials Science and Engineering Laboratory
National Institute of Standards and Technology
100 Bureau Dr. Stop 8520
Gaithersburg, MD 20899-8520

L. Swartzendruber, H. J. Brown
Division of Metallurgy, Materials Science and Engineering Laboratory
National Institute of Standards and Technology
100 Bureau Dr. Stop 8552
Gaithersburg, MD 20899-8552

David T. Shaw
330 Bonner Hall
State Univ. of New York at Buffalo
Amherst, NY 14260-1900

ABSTRACT

Efforts to improve the magnetic flux-pinning properties of $Bi_2Sr_2CaCu_2O_{8+\delta}$/Ag (2212/Ag) tape conductors utilizing $(Sr_{1-x}Ca_x)_{14}Cu_{24}O_{41+\delta}$ and $Sr_2CaAl_2O_6$ defects are described. Precursor powders with composition (2212 + N% volume fraction $Sr_{10}Ca_4Cu_{24}O_{41+\delta}$; N = 0, 7, 15) were prepared by solid-state reaction to obtain subsolidus phase equilibrium at 860°C, as measured by X-ray diffraction (XRD). Nanophase (10 – 20 nm) Al_2O_3 was added (1.1% mass fraction) to N = 0 and 15 fully reacted powders. Brush-on coated tapes (13 – 17 μm 2212 thickness) were processed by a partial-melt growth method in air with variable melting from 865°C to 890°C, and slow-cool recrystallization from 856°C to 847°C. The effect of different melt temperatures and compositions on film properties (phase assemblages, orientations, and compositions, and defect sizes) was studied by XRD, scanning electron microscopy (SEM), and energy dispersive spectroscopy (EDS). Higher N increased the amount of $(Sr_{1-x}Ca_x)CuO_{2+\delta}$ and $(Sr_{1-x}Ca_x)_{14}Cu_{24}O_{41+\delta}$ defects observed in processed films.

Addition of 1.1% mass fraction Al_2O_3 for N = 0, 15 powders and melt temperatures (870 – 900°C) had two main effects: (1) Al_2O_3 reacted within ≤ 0–4 minutes of melting to produce defects with primary composition $Sr_2CaAl_2O_{6+\delta}$, as verified by XRD and EDS, and (2) dramatically shifted the phase assemblages toward increasing $(Sr_{1-x}Ca_x)_{14}Cu_{24}O_{41+\delta}$ and decreasing $(Sr_{1-x}Ca_x)CuO_{2+\delta}$ defects. The $Sr_2CaAl_2O_6$ defects increased to 1–5 μm size by coarsening with increasing melting temperatures (~880–895°C). Magnetic critical current density (J_c) of (N=15+alum powder) tapes showed improvement for 1T applied fields in the 20–30 K range. Transport J_c (4.2K, 0T) of N=15 and N=15+alum composition tapes were ~30% and ~5%, respectively, of N=0 tapes.

INTRODUCTION

Practical conductors of $Bi_{2+x}Sr_{2-x-y}Ca_{1+y}Cu_{2+z}O_{8+\delta}$/Ag are excellent candidates for long length high current and power applications because of their ability to be fabricated by lower-cost methods, and their high transport J_cs in reasonable magnetic fields.[1,2] Because of intrinsically poor flux-pinning, the expected operation temperature for Bi-2212 conductors is <50K for parallel magnetic fields[3] and <30K for perpendicular magnetic fields.[2,3] The limit for practical applications is generally referred to in temperature - magnetic field space by the "irreversible" or "melting" line, above which superconductivity is destroyed.[2] However with the creation of pinning defects (by irradiation), the irreversibility line of Bi-2212 was shifted ~20°K higher in tapes or crystals, and the magnetic J_c at all temperatures and magnetic fields was improved.[2,4]

In this paper, two methods for creating solid non-superconducting flux-pinning defects were explored. In the first method, an off-stoichiometric powder was used to increase formation of $(Sr_{14-x}Ca_x)Cu_{24}O_{41+\delta}$ (014x24) defects in subsolidus powders and melt-processed tapes. In the second method, the reaction of nanophase Al_2O_3 with Bi-2212 melts to create non-superconducting defects was studied.

To our knowledge, there has been no attempt thus far to add 014x24 defects to 2212 composition tapes. The 014x24 defect typically forms instantaneously upon melting by peritectic decomposition,[5-7] therefore it is analogous to the formation of Y_2BaCuO_5 (211) defects in $YBa_2Cu_3O_{7+\delta}$ (YBCO).[8] By analogy to 211 defect pinning in YBCO, it should be possible to increase $J_c(H)$ of Bi-2212 by controlling the size and density of 014x24 defects; i.e. $J_c \sim V_f/d$, where V_f is the volume fraction of defects and d is the defect size.[8] This paper examines how to increase V_f/d of 014x24 defects by changing the composition (to increase V_f), and by addition of nanophase particles and precise timing of the melt (to reduce 014x24 coarsening and particle size).

The addition of nanophase Al_2O_3 to Bi-2212 melted pellets showed improvement for flux-pinning,[9] however there is no report in the literature to our

knowledge on improvement for flux-pinning of Bi-2212 films. Nanophase Al_2O_3 was used to reduce $(Sr_{1-x}Ca_x)CuO_{2+\delta}$ (01x1) defect formation in Bi-2212 isothermal melt processing.[10] The reaction products of Al_2O_3 and Bi-2212 melts were measured approximately by several groups.[9,10]

Solid phases identified in this work are shown in Table I. All of the phases exist as solid-solutions, where Ca can substitute for Sr in the lattice structures. Several of the phases formed during melt growth had Sr:Ca ~2:1, which was close to the Sr:Ca composition of the melts.

Table I. Chemical Phases and Corresponding Symbols in this study.

Chemical Formula	Symbol
$Bi_{2+x}Sr_{2-x-y}Ca_{1+y}Cu_{2+z}O_{8+\delta}$	2212
$Bi_{2+x}Sr_{2-x-y}Ca_yCu_{1+z}O_{6+\delta;}$ x = 0.1 to 0.4	2201-R
$(Sr_{14-x}Ca_x)Cu_{24}O_{41+\delta}$; x = 0 to 7 *	014x24
$(Sr_{1-x}Ca_x)CuO_{2+\delta}$; x = 0 to 0.75	01x1
$Bi_2Sr_{3.9-x}Ca_xO_{9-\delta}$; x ≅ 0.5 to 1.7 *	24x0
$(Sr_2Ca)Al_2O_{6+\delta}$ *	$03Al_2$

* Sr:Ca ~2:1 in melt-processed films

EXPERIMENTAL**

Precursor powders were prepared by the solid-state method, using starting reactants of Bi_2O_3, $SrCO_3$, $CaCO_3$, and CuO (≥ 99.95% purity). Powders were mixed and ground with mortar and pestle, calcined by slow heating 650°C to 830°C at 25°C/h, and subsequent annealing and intermediate grinding at 830°C to 860°C. Powders were annealed in air until phase equilibrium was reached (~3-4 annealings) at 860°C, as determined by X-ray diffraction (XRD). The powders were reacted in ~1 cm diameter pellets (0.8 – 1 g batches), formed by lightly pressing (~5-10x10^6 Pa) in molds. The slow-heating calcination step was used to eliminate intermediate melting reactions[5] of the sacrificial powder with the polycrystalline MgO pellet support substrates. Three powders of composition ($Bi_2Sr_2CaCu_2O_{8+\delta}$ + N% volume fraction $Sr_{10}Ca_4Cu_{24}O_{41+\delta}$, N = 0, 7 and 15) were prepared, as shown in Table II. Two additional powders (Table II) were made by mixing 1.1% mass fraction[10] (~1.8% volume fraction) 10-20 nm size Al_2O_3

** "Certain commercial equipment, instruments, or materials are identified in this paper in order to specify the experimental procedure adequately. Such identification is not intended to imply recommendation or endorsement by the National Institute of Standards and Technology, nor is it intended to imply that the materials or equipment identified are necessarily the best available for the purpose."

(99.98%, gamma-alpha, density = 3.965 g/cm^3) powder purchased commercially[11] to N = 0 and 15 fully reacted powders. The $Sr_{10}Ca_4Cu_{24}O_{41+\delta}$ composition of the solid-solution 014x24 phase was chosen based on observations of 014x24 composition in melt-quenched tapes using B1 powder partially reacted.[5,6]

Table II. Powder compositions tested in this study.

Symbol	Composition	Powder Subsolidus Phases (860°C)	Processed Film XRD Phases (890-895°C)
B1	2212 ($Bi_2Sr_2Ca_1Cu_2O_{8+\delta}$)	2212 24x0, x ~1.5	2212 01x1, x ~0.5 * 014x24, x ~7 * 2201-R * 24x0, x ~1.3
B2	B1 + 7% volume fraction 014x24, x = 4 ($Bi_2Sr_{2.16}Ca_{1.07}Cu_{2.39}O_{9-\delta}$)	2212 24x0, x ~1.5 014x24, x = 4	2212 01x1, x ~0.5 * 014x24, x ~7 2201-R * 24x0, x ~1.3
B3	B1 + 15% volume fraction 014x24, x = 4 ($Bi_2Sr_{2.38}Ca_{1.15}Cu_{2.92}O_{10-\delta}$)	2212 24x0, x ~1.0 014x24, x = 4	2212 01x1, x ~0.4 * 014x24, x ~5 2201-R * 24x0, x ~1.3
B1+alum	B3 + 1.1% mass fraction 10-20 nm size Al_2O_3		2212 01x1, x ~0.5 * 014x24, x ~5-7 2201-R * 24x0, x ~1.3 $03Al_2$*
B3+alum	B3 + 1.1% mass fraction 10 – 20 nm size Al_2O_3		2212 01x1, x ~0.5 * 014x24, x ~5 2201-R * 24x0, x ~1.3 $03Al_2$*

* secondary phases not observed in precursor powder

Thick film tapes were made by adding ~30 mg of powder to ~0.5 ml 200 proof alcohol, and brush-coat depositing onto Ag foil (99.9%, 0.0050 cm thick). Powders were stored in a dry-box with desiccant, to avoid long-term chemical reactions with solvents and moisture. The film thickness was controlled from 13 μm to17 μm to keep XRD film peak intensities consistent.

The partial-melt processing profile used is shown in Figure 1. In Figure 1, only T_{max} was varied (shown with several examples) and the recrystallization temperature range (856°C to 847°C)[5,12] was held constant. The heating and cooling rates to/from ~845°C are comparable to rates that can be achieved with large-scale processing furnaces. The cooling rate below 847°C was furnace cooling (847°C to 500°C at ~120°C/h and 500°C to 40°C at ~60°C/h).

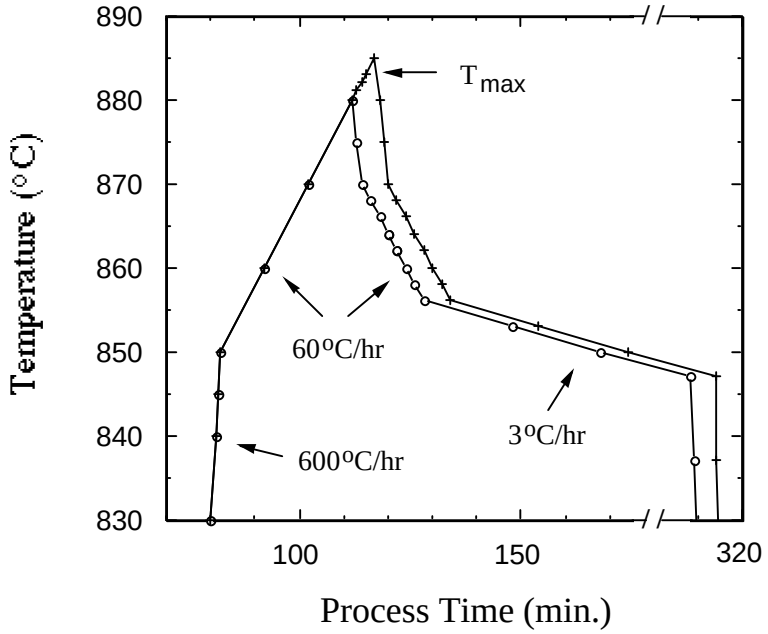

Figure 1. Partial-melt growth temperature-time process profile, showing examples for different T_{max} (+ T_{max} = 885°C, ∘ T_{max} = 880°C)

X-ray diffraction was performed with Philips diffractometers with 12 mm optics and theta compensating slits and automated with the use of Radix Databox interfaces. Two-theta calibrations for XRD scans were made using LaB_6 powder. A 2θ step-size of 0.03Å and a count time per step of 2 s was used. Energy dispersive X-ray spectroscopy (EDS) was measured using conventional methods with data reduction via the DTSA software package.[13,14] Standards for EDS analysis were $Bi_2Sr_{1.5}Ca_{1.5}Cu_2O_x$ and corundum. Particle analysis software (NIH-

Image 1.60) was used to determine the surface volume percentage of needle and $03Al_2$ defects.

Magnetic J_c was measured with a SQUID magnetometer (Quantum Design, MPMS/MPMS^2). Rectangular shaped tapes were placed in low magnetic response organic sample holders with the tape surface oriented perpendicular to the applied magnetic field. M-H hysteresis loops at different temperatures were made by warming samples to 100K and zero-field cooling (ZFC) to measurement temperature.[8] Magnetic J_cs were calculated using the extended Bean critical current model $J_c = 20\Delta M*3b/(a(1-a))$, where ΔM is the magnetic hysteresis difference, and a and b are the dimensions of the tape rectangle.[15] The difference between positive and negative magnetic field ΔM measurements were compared, and the difference was normally <1%, except near the limit as ΔM approached 0. Transport J_cs were made with a four-contact method using a 1 μV/cm criteria.

Temperatures used for processing were measured at reaction sites with S-type thermocouples calibrated with gold melting (~1-2^{o}C accuracy).

RESULTS

2212 + 014x24 Addition

Table I indicates phases in subsolidus equilibrium powders and processed films made with the powders, as identified by XRD. A comparison of B1, B2 and B3 powders indicate the subsolidus phase assemblage did not change with 014x24 defect addition, except that increasing 014x24 phase was observed. This indicates that the tie-plane region between the solid-solution 2212 and 014x24 phases in Bi-Sr-Ca-Cu-O quaternary phase space exists in equilibrium at 860^{o}C. This observation is consistent with previous studies, where the 014x24 phase was observed in four-phase subsolidus equilibrium tetrahedra regions up to the melting temperatures of the compositions.[16]

Phases in processed films were similar to phases in subsolidus powders, however additional phases were observed because of the non-equilibrium melting process. The 01x1 and 014x24 phases were observed with large size with XRD and SEM, and a small amount of 24x0 and 2201-R was observed by XRD. The Sr:Ca ratio of the 014x24 and 24x0 phases shifted towards Sr:Ca ~2:1 in films compared to powders, except for slight shifts of 014x24 phase in B1 and B2 films.

Figure 2 shows XRD intensities of unique peaks of 2212, 01x1, 014x24 and $03Al_2$ phases from tapes made with every composition listed in Table II. The films in Figure 2 were optimized for 2212 intensity at T_{max} = 890^{o}C to 895^{o}C. At lower T_{max} temperature, the 2212 intensity was ~50-65% lower for B3, B1+alum, and B3+alum tapes (however not B1 tapes). The peak used for $03Al_2$ identification ($2\theta = 32.44^o$) is preliminarily identified as the (440) reflection, similar to the highest intensity peak in $Sr_3Al_2O_6$ and $Ca_3Al_2O_6$.[17,18]

As the powder composition was varied for increasing N% of 014x24 addition, the 01x1 and 014x24 XRD intensities increased in processed tapes, as expected. Also in Figure 2 the 2212 phase XRD intensity for B3 and B+alum tapes is reduced ~65-70% compared to tapes with B1 powder. This is predicted to some extent, as a higher percentage of the surface is covered with defects (Fig. 3 and 4). The surface area of defects for tapes in Figures 3 and 4 are: B1 ~4%, B3 ~17%, B1+alum ~28%, B3+alum ~15%; which includes ~3% $03Al_2$ phase for B+alum films.

For B3 powder tapes, the surface area (~volume fraction) of defects achieved (~17%) was close to what was expected from the precursor powder composition (~15% volume fraction 014x24). However the needle defect size was much larger than considered optimal for flux-pinning (Fig. 3). Only at low melting temperatures (T_{max} ~872.5°C) was a large amount of smaller defects (~1–5 μm size) observed. However at T_{max} = 872.5°C the 2212 XRD intensity for B3 tapes was only ~25% of the value achieved at 895°C, which suggests poor 2212 c-axis alignment or phase structure.

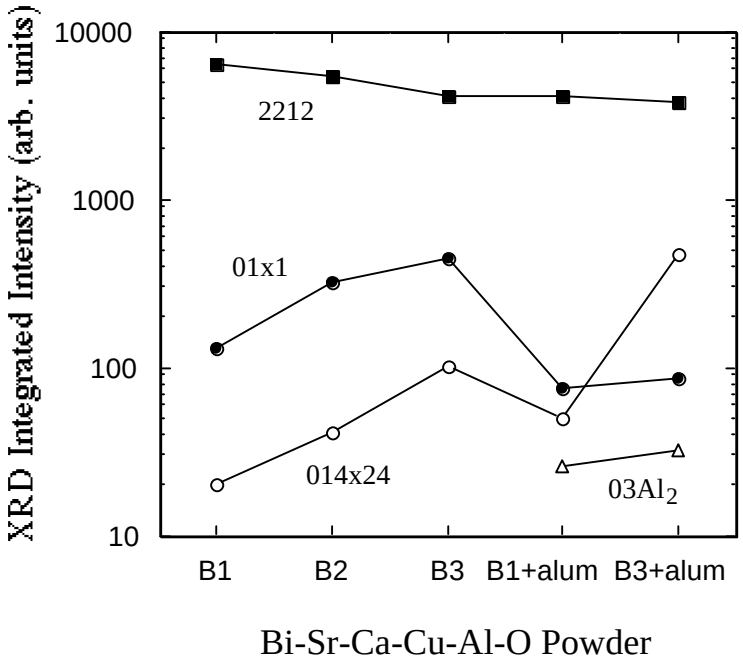

Figure 2. XRD film peak intensities of the (008) peak of 2212, (040) peak of 014x24, (110) peak of 01x1, and (440) peak of $03Al_2$; from films processed with range T_{max} = 890°C to 895°C.

2212 + Al_2O_3 Addition

Table II and Figure 2 indicate that when nanophase Al_2O_3 was added to B1 and B3 powders, a reaction product $03Al_2$ was observed with both EDS and XRD in processed films. The composition as determined by EDS contained a slight (~2-4%) amount of both Bi and Cu in it, however this could result from secondary X-ray scattering from the matrix surrounding the defect particle. Several new 2θ peaks (32.44^o, 40.01^o and 46.56^o) in XRD scans were observed in B+alum films, which matched precisely the 2θ high intensity peaks of a powder sample of $Sr_2CaAl_2O_6$ prepared by solid-state reaction at 1325^oC for about 10 days.

The onset temperature for $03Al_2$ phase formation in the melt was T_{max} ~870^oC for B1+alum and B3+alum tapes. The onset of 2212 c-axis orientation (corresponding to melting) for B1+alum was T_{max} ~870^oC and for B3+alum was T_{max} ~866^oC. Therefore the reaction of Al_2O_3 and the melt occurred faster for

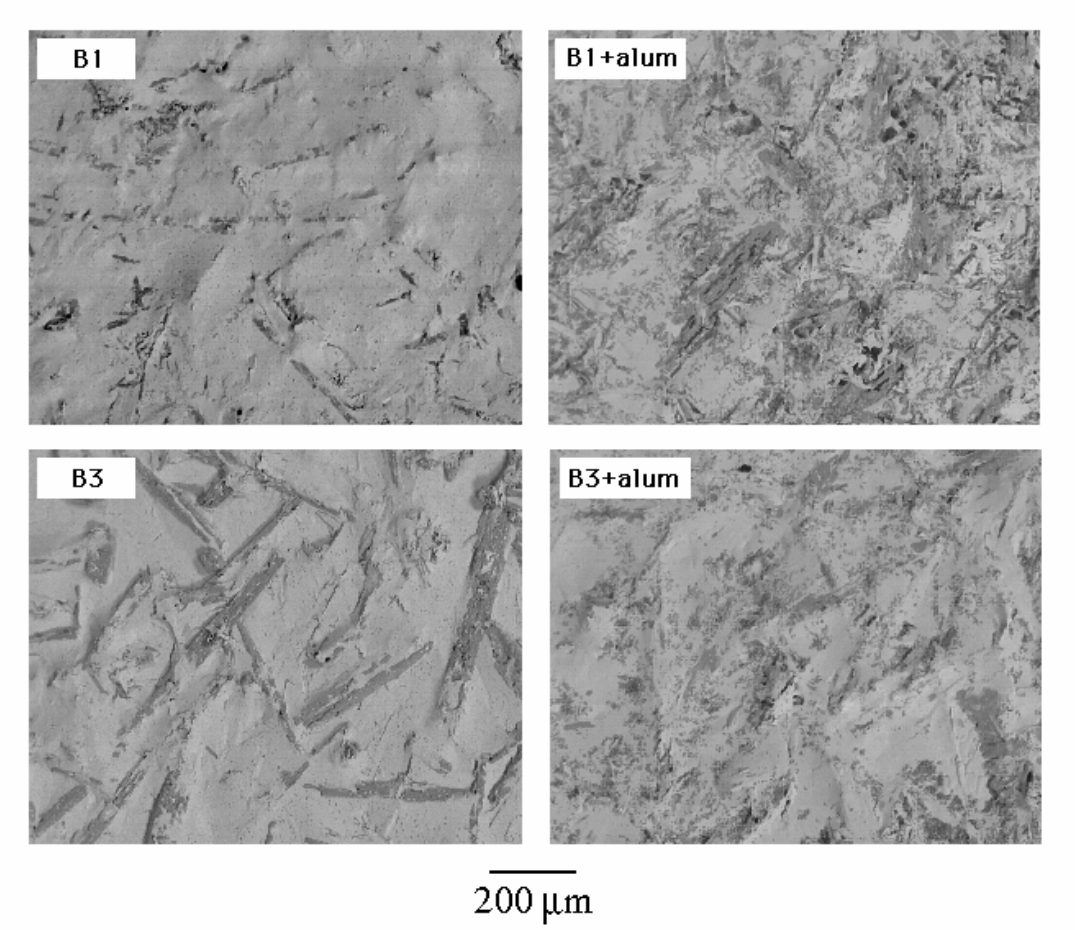

Figure 3. SEM micrographs of films processed with range T_{max} = 890 - 895^oC.

B1+alum powder (≤ 0 minutes) than for B3+alum powder (~4 min). The reaction of $03Al_2$ was complete by T_{max} = 873°C to 875°C for B3+alum powder, as determined by XRD intensity of the (440) peak.

The 2θ values for the $03Al_2$ phase did not shift measurably for T_{max} = 870°C - 900°C for B1+alum and B3+alum films, which is strong indication that the composition is stable for different melting temperatures and powder compositions. X-ray diffraction was useful for identifying the $03Al_2$ phase in tapes where the particle size was too small to easily detect using backscattered SEM imaging (T_{max} ~870 –880°C).

The reaction product of Al_2O_3 and Bi-2212 melts identified in this work ($03Al_2$) is different in composition from previous studies where the reaction product was approximately identified as $(Sr_{2-x}Ca_x)AlO_y$ or $(Bi_2Sr_{4-x}Ca_x)Al_3O_y$[10] or

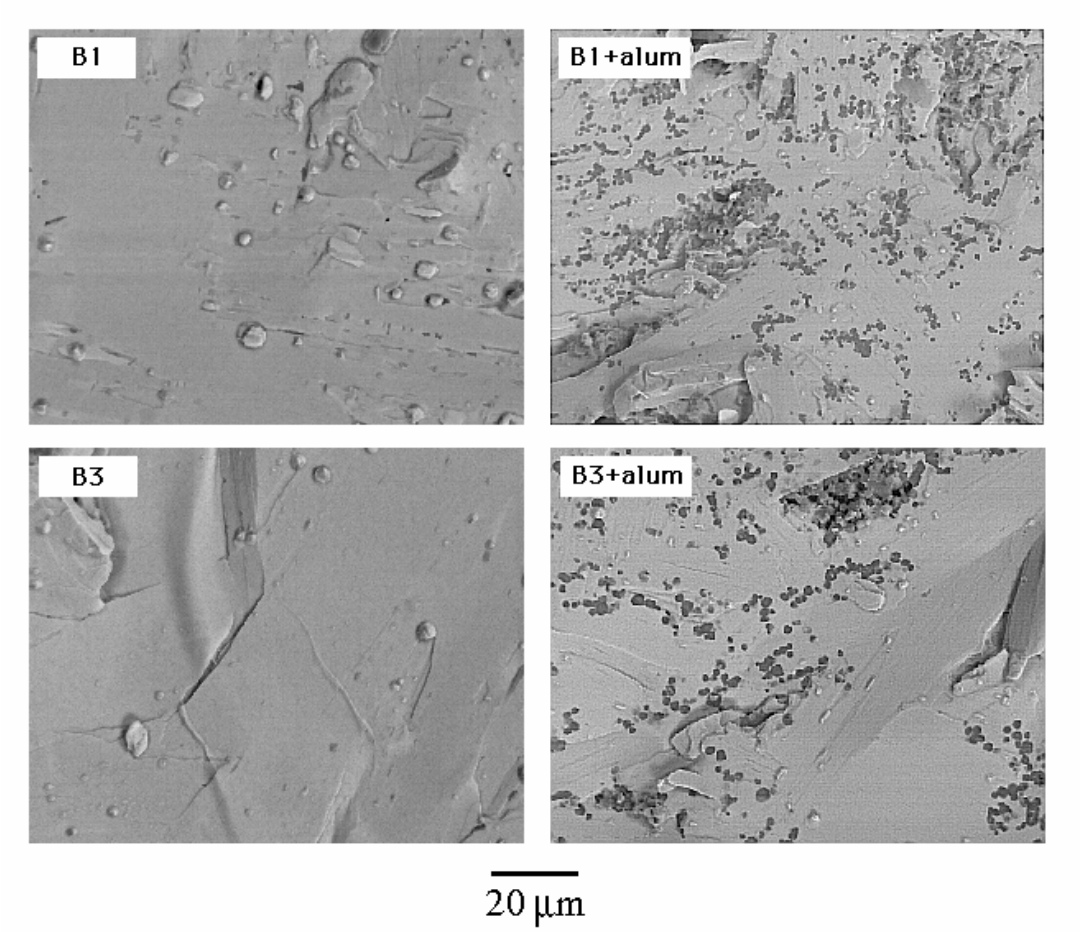

Figure 4. High magnification SEM micrographs of films processed with range T_{max} = 890°C to 895°C. Darker phase defects in B+alum films are $03Al_2$ phase.

$BiSr_{1.5}Ca_{0.5}Al_2O_x$[9]. The different reaction products observed may result from varying powder or film processing conditions; i.e. in Ref [10] the precursor powder was prepared as an amorphous glass, where Bi may be more reactive than in the present study, and in Ref [9] micron-sized Al_2O_3 was reacted with different composition Bi-2212 pellets melted ~2-3 hrs (slow-cool 10°C/h from 885°C) prior to recrystallization.

As shown in Figure 3 for B3 and B3+alum tapes, the addition of nanophase alumina had some effect for reducing large needle defect formation. However interestingly, for B1 powder the addition of 1.1% mass fraction of nanophase Al_2O_3 alumina created a disproportionately larger amount of surface defects (~28% for B1+alum, compared to ~4% for B1). This indicates the 2212 phase is sensitive to Bi:Sr:Ca:Cu composition for creating surface defects in films.

Finally, Figure 4 shows the $03Al_2$ particle size grew by coarsening and coalescence to ~1-5 μm at T_{max} = 890–895°C. Even larger $03Al_2$ particles (~5-10 μm) are observed in Figure 4 at the beginning stages of formation.

Critical Current Density

Figure 5 shows magnetic J_c for B3+alum tapes (Fig. 3) and B1[4] powder tapes processed at ~880-895°C. Magnetic J_c(5K, 0T) for tapes in Figure 5 were B1 ~$1.0x10^5$ A/cm^2 [Ref. 4] and B3+alum ~30,000 A/cm^2. The J_c properties for

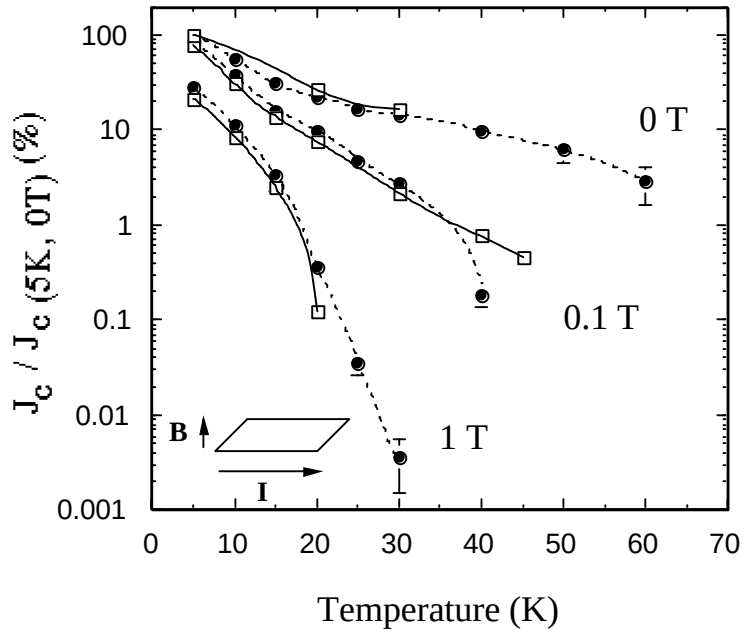

Figure 5. Magnetic J_c for B3+alum film processed with T_{max} = 880°C and 895°C (•) and B1 (□)[4] powder tapes. Error bars indicate range of variation for different T_{max}.

B3+alum in Figure 5 were consistent for tapes processed with different maximum temperature (T_{max} = 880 and 895°C). The magnetic J_c shows improvement at 20 – 30K in a 1T applied magnetic field.

Transport J_c(4.2K, 0T) for sample tapes with different composition were B1 ~50,000 A/cm^2, B3 ~13,000 A/cm^2, and B3+alum ~2500 A/cm^2. A significant drop of transport J_c is expected for B3 compared to B1 tapes, as the needle structure is quite large (Fig. 3) which restricts current flow. However it's unclear yet why B3+alum tapes had very low transport J_c (~5% of B1 tapes), as the magnetic J_cs were ~30-50% of B1 tapes. No measurable amount of Al was incorporated into 2212 composition areas to the limit of EDS measurements, consistent with previous observations.[10]

CONCLUSIONS

Partial-melt processing of ($Bi_2Sr_2Ca_1Cu_2O_{8+\delta}$ + N% volume fraction $Sr_{10}Ca_4Cu_{24}O_{41+\delta}$; N = 0, 7, 15) thick film conductors showed increasing 014x24 and 01x1 defects for increasing N. Higher 014x24 phase content (and lower 01x1 phase content) could be achieved by adding 1.1% mass fraction 10 – 20 nm size Al_2O_3 particles. Smaller 014x24 defect size (~1-5 μm) was achieved at ~872.5°C melt temperature (T_{max}), whereas optimal 2212 film XRD intensity was achieved at T_{max} ~890–895°C. Nanophase Al_2O_3 reacted with 2212 melts within ≤ 0-4 min (T_{max} ≥ 870°C) of melting to produce defects with primary composition $Sr_2CaAl_2O_{6+\delta}$, as verified by XRD and EDS. The reaction product ($03Al_2$) had unchanging 2θ peak positions for all melting temperatures (T_{max} ~870–900°C) tested for a given composition (N = 0,15), however the $03Al_2$ defects increased in size to ~1–5 μm by coarsening with increasing melting temperatures (~880-895°C). Magnetic critical current density (J_c) of (N=15+alum powder) tapes showed improvement for 1T applied fields in the 20–30 K range. Transport J_c (4.2K, 0T) of N=15 and N=15+alum composition tapes were ~30% and ~5%, respectively, of N=0 tapes.

ACKNOWLEDGEMENTS

The authors would like to thank T. Francavilla of Naval Research Laboratory for assistance with transport J_c measurements.

REFERENCES

[1]M. S. Walker, D. W. Hazelton, M. T. Gardner, J. A. Rice, D. G. Walker, C. M. Trautwein, N. J. Ternullo, Z. Shi, J. M. Weloth, R. S. Sokolowski, and F. A. List, "Performance of Coils Wound from Long Lengths of Surface-Coated, Reacted, BSCCO-2212 Conductor," IEEE Trans. Appl. Supercond., 7[2] 889-892 (1997).

[2]D. T. Shaw and S. Jin, "Ceramic Processing and Wire Fabrication of High T_c Superconductors"; pp. 87 – 120, in *Processing and Properties of High T_c Superconductor*s *Volume 1. Bulk Materials*, Edited by S. Jin (World Scientific Publishing Co. Pte. Ltd., NJ 1993).

[3]H. Kumakura, K. Togano, H. Kitaguchi, H. Maeda, and J. Kase, "Critical Current Density and Flux Pinning in Textured $Bi_2Sr_2CaCu_2O_8$ Tapes," Physica C, 185-189 2341-2342 (1991).

[4]L. Krusin-Albaum, J. R. Thompson, R. Wheeler, A. D. Marwick, C. Li, S. Patel, D. T. Shaw, P. Lisowski and J. Ullman, "Enhancement of persistent currents in $Bi_2Sr_2CaCu_2O_8$ tapes with splayed columnar defects induced with 0.8 GeV protons," Appl. Phys. Lett., 64 3331-3333 (1994).

[5]T. Haugan, *Partial-Melt Growth of $Bi_2Sr_2CaCu_2O_{8+d}$/Ag Superconducting Tapes*, Ph.D. Dissertation, State Univ. of New York at Buffalo (UMI Dissertation Services, Ann Arbor MI, U.S.A. 1995).

[6]T. Haugan, J. Ye, S. Chen, S. S. Li, S. Patel, and D. T. Shaw, "Growth of $Bi_2Sr_2CaCu_2O_x$ /Ag Single Layer and Multilayer Superconducting Tape Systems"; pp 609-615, in *Superconductivity and Its Applications Buffalo, NY 1992*, Edited by H. S. Kwok et. al., AIP Conf. Proc. 273 (AIP, NY 1993).

[7]J. Kase, K. Togano, H. Kumakura, D. R. Dietderich, N. Irisawa, T. Morimoto, H. Maeda, "Partial-Melt Growth Process of $Bi_2Sr_2CaCu_2O_x$ Textured Tapes on Silver," Jpn J. Appl. Phys. 29 L1096-L1099 (1990).

[8]M. Murakami, "Melt Processing, Flux Pinning and Levitation"; pp. 213–272, in *Processing and Properties of High T_c Superconductor*s *Volume 1. Bulk Materials*, Edited by S. Jin (World Scientific Publishing Co. Pte. Ltd., NJ 1993).

[9]K. C. Goretta, V. R. Todt, D. J. Miller, M. T. Lanagan, Y. L. Chen and U. Balachandran, "Engineered Flux-Pinning Centers in $Bi_2Sr_2CaCu_2O_x$ and $TlBa_2Ca_2Cu_3O_x$ Superconductors," J. Electron. Mater. 24 1961-1966 (1995).

[10]T. G. Holesinger, "Al_2O_3 additions for isothermal melt processing of $Bi_2Sr_2CaCu_2O_y$," J. Mater. Res. 11[9] 2135-2141 (1996).

[11]Alfa-Aesar, 30 Bond Street, Ward Hill, MA 01835.

[12]T. Haugan, S. Patel, J. Pitsakis, F. Wong, S. J. Chen, D. T. Shaw, "Recent Status on High Temperature Superconducting $Bi_2Sr_2CaCu_2O_{8+x}$ Wire Development at NYSIS: 1-90 Meter Length J_cs and 3 Meter Diameter Ring Furnace Design," J. Electron. Mat. 24[12] 1811-1815 (1995).

[13]K. F. J. Heinrich, *Electron Beam X-ray Microanalysis*, p. 578 (Van Nostrand Reinhold Co., New York, 1981).

[14]C. E. Fiori, C. R. Swyt, and R. L. Myklebust, "NIST/NIH Desktop Spectrum Analyzer Program and X-ray Database", NIST Standard Reference Database No. 36, National Institute of Standards and Technology, Gaithersburg, MD (1991).

[15]M. Muralidhar, M. R. Koblischka, and M. Murakami, "Refinement of secondary phase particles for high critical current densities in (Nd,Eu,Gd)-Ba-Cu-O superconductors," Physica C 313 232-240 (1999).

[16]W. K. Wong-Ng, L. P. Cook, "Melting Equilibria of the Bi-Sr-Ca-Cu-O (BSCCO) System in Air: The Primary Crystallization Phase Field of the 2212 Phase and the Effect of Silver Addition," J. Am. Ceram. Soc. 81[7] 1829-1838 (1998).

[17]W. Wong-Ng, H. F. McMurdie, B. Paretzkin, Y. Zhang, K L. Davis, C. R. Hubbard, A. L. Dragoo, and J. Stewart, "Standard X-ray Diffraction Powder Patterns of Sixteen Ceramic Phases," Powder Diffraction 2 [3] 191– 202 (1987).

[18] H. Swanson, H. McMurdie, M. Morris, E. Evans, and B. Paretzkin, "Standard X-ray Diffraction Patterns Section 10 – Data for 84 Substances," National Bureau Standards (U. S.) Monograph 25 [10] 51-52 (1972).